0026-895X/05/6703-883–890$20.00
MOLECULAR PHARMACOLOGY
Copyright © 2005 The American Society for Pharmacology and Experimental Therapeutics
Mol Pharmacol 67:883–890, 2005

Vol. 67, No. 3
4523/1195621
Printed in U.S.A.

Optimized Targeting of Polyethylene Glycol-Stabilized Anti-Intercellular Adhesion Molecule 1 Oligonucleotide/Lipid Particles to Liver Sinusoidal Endothelial Cells

Martin Bartsch, Alida H. Weeke-Klimp, Henriëtte W. M. Morselt, Andrea Kimpfler, Sigridur A. Ásgeirsdóttir, Rolf Schubert, Dirk K. F. Meijer, Gerrit L. Scherphof, and Jan A. A. M. Kamps

Groningen University Institute for Drug Exploration (GUIDE), Department of Cell Biology (M.B., A.H.W.-K., H.W.M.M., G.L.S., J.A.A.M.K.), Pathology and Laboratory Medicine/Medical Biology (H.W.M.M., S.A.A., J.A.A.M.K.), Pharmacokinetics and Drug Delivery (D.K.F.M.), University of Groningen, The Netherlands; and the Department of Pharmaceutical Technology, University of Freiburg, Germany (A.K., R.S.).

Received July 2, 2004; accepted December 10, 2004

ABSTRACT

We prepared polyethylene glycol (PEG)-stabilized antisense oligonucleotide (ODN)/lipid particles from a lipid mixture including the positively charged amphiphile 1,2-dioleoyl-3-trimethylammonium-propane (DOTAP) and anti-intercellular adhesion molecule 1 (ICAM-1) antisense ODN by an extrusion method in the presence of 40% ethanol. These particles were targeted to scavenger receptors on liver endothelial cells by means of covalently coupled polyanionized albumin. Two types of such targeted particles were prepared, one with the albumin coupled to a maleimide group attached to the particle's lipid bilayer and the other with the protein coupled to a maleimide group attached at the distal end of added bilayer-anchored PEG chains. Upon intravenous injection, the ODN particles with bilayer-coupled albumin were cleared from the blood circulation at the same low rate as untargeted particles (<5% in 30 min). By contrast, the distal-end coupled particles were very rapidly cleared from the blood and preferentially taken up by the endothelial cells of the hepatic sinusoid (55% of injected dose after 30 min). Despite this substantial endothelial targeting, no consistent inhibition of ICAM-1 expression could be demonstrated in this cell type, either in vivo or in vitro. However, in J774 cells that also express scavenger receptors and ICAM-1, significant down-regulation of ICAM-1 mRNA was achieved with distal-end targeted lipid particles, as determined with real-time RT-PCR. It is concluded that massive delivery of ODN to cell types that express scavenger receptors can be achieved if lipid particles are provided with negatively charged albumin distally attached to bilayer anchored PEG chains.

Antisense oligonucleotides (ODN), by virtue of their ability for sequence-specific down-regulation of mRNA synthesis, provide a potentially powerful tool to modulate gene expression both in vitro and in vivo (Matteucci and Wagner, 1996). For this reason, there is a great interest in the clinical application of ODN as experimental drugs. This is reflected by the large number of clinical trials under way for a variety of clinical conditions including cardiovascular, inflammatory and infectious diseases, organ transplantation, and cancer (Kurreck, 2003). In these trials, only so called "naked" ODN formulations have been employed (Opalinska and Gewirtz, 2002; Pirollo et al., 2003). It is generally recognized, however, that further exploitation of ODN therapy requires the development of target-specific ODN formulations (Scherer and Rossi, 2003; Allen and Cullis, 2004).

We succeeded previously in the efficiently targeted delivery of liposomes to liver endothelial cells in vivo by exploiting the high affinity of aconitylated human serum albumin (Aco-

This study was supported by the Netherlands Research Council for Chemical Sciences (CW) with financial aid from the Netherlands Technology Foundation (grant 349-4757).
Article, publication date, and citation information can be found at http://molpharm.aspetjournals.org.
doi:10.1124/mol.104.004523.

ABBREVIATIONS: ODN, oligonucleotide; HSA, human serum albumin; Aco-HSA, *cis*-aconitic anhydride-modified human serum albumin; PEG, polyethylene glycol; CCL, coated cationic lipoplex; SALP, stabilized antisense lipid particle; PEG-DSPE, 1,2-distearoyl-*sn*-glycero-3-phosphoethanolamine-*N*-[methoxy(polyethylene glycol)-2000]; Mal-PEG-DSPE, 1,2-distearoyl-sn-glycero-3-phosphoethanolamine-*N*-[methoxy(polyethylene glycol)-2000]-maleimide; POPC, 1-palmitoyl-2-oleoyl-*sn*-glycero-3-phosphocholine; MPB-PE, 1,2-dioleoyl-*sn*-glycero-3-phosphoethanolamine-*N*-[4-(*p*-maleimidophenyl)butyramide]; DOTAP, 1,2-dioleoyl-3-trimethylammonium-propane; [^{3}H]COE, [1α,2α(n)-^{3}H]cholesteryl oleyl ether; PS, phosphatidylserine; rr, recombinant rat; IL, interleukin; TNF, tumor necrosis factor; IFN, interferon; TL, total amount of lipid; HBS, HEPES-buffered saline; EC, endothelial cell; PCR, polymerase chain reaction; RT, reverse transcription; C_T, threshold cycle; ScR, scavenger receptor.

HSA) for scavenger receptors on these cells, whereas with unmodified HSA, uptake of liposomes by the liver was low (<10%) (Kamps et al., 1996, 1997). Using this targeting principle, we were also able to target antisense ODN encapsulated in polyethylene glycol (PEG) bearing coated cationic lipoplexes (CCLs) to the endothelial cell population of the liver (Bartsch et al., 2002). Semple et al. (2001) and Stuart et al. (2004) described the preparation of an alternative ODN encapsulating stabilized antisense lipid particle (SALP), grafted with polyethylene glycol, potentially suitable for in vivo applications. In vitro, SALPs could be targeted to the folate receptor on KB cells, a cell line derived from a human epithelial carcinoma, by introducing folate-PEG coupled to a lipid anchor (Zhou et al., 2002). In our previous experiments, we coupled the targeting device (Aco-HSA) directly to the bilayer by a lipid-anchored maleimide group (Kamps et al., 1997; Bartsch et al., 2002). Development of polyethylene glycol polymers with maleimide modifications (Mal-PEG-DSPE) at the distal end allows the covalent coupling of targeting ligands to the distal end of PEG chains. We compared the in vivo targeting efficiency of SALP particles containing an anti-ICAM-I ODN sequence with a targeting device (Aco-HSA), coupled either directly to the bilayer or to the distal end of bilayer-anchored PEG chains and determined their ability to modulate ICAM-I mRNA levels.

Materials and Methods

Chemicals. 1-Palmitoyl-2-oleoyl-*sn*-glycero-3-phosphocholine (POPC), 1,2-dioleoyl-*sn*-glycero-3-phosphoethanolamine-*N*-[4-(*p*-maleimidophenyl)butyramide] (MPB-PE), 1,2-distearoyl-*sn*-glycero-3-phosphoethanolamine-*N*-[methoxy(polyethylene glycol)-2000]-maleimide (Mal-PEG-DSPE), 2-distearoyl-*sn*-glycero-3-phosphoethanolamine-*N*-[methoxy(polyethylene glycol)-2000], 1,2-dioleoyl-3-trimethylammonium propane (DOTAP), and bovine brain phosphatidylserine (PS) were purchased from Avanti Polar Lipids (Alabaster, AL). [1α,2α(n)-^{3}H]cholesteryl oleyl ether ([^{3}H]COE), was from Amersham Biosciences (Little Chalfont, Buckinghamshire, UK). Cholesterol, *N*-succinimidyl-*S*-acetylthioacetate, *cis*-aconitic anhydride, and DEAE-Sepharose CL-6B were from Sigma-Aldrich (St. Louis MO). Human serum albumin fraction V (HSA) was obtained from the Central Laboratory of the Red Cross (Amsterdam, The Netherlands). OliGreen reagent was purchased from Molecular Probes, Inc. (Leiden, The Netherlands). Pronase (from *Streptomyces griseus*) and collagenase A were obtained from Roche Diagnostics (Mannheim, Germany). Recombinant rat (rr) and recombinant murine interleukin-1β (IL-1β), tumor necrosis factor α (TNF-α), and interferon-γ (IFN-γ) were purchased from R&D Systems, Inc. (Minneapolis, MN). All other chemicals were analytical grade or the highest grade available.

Antisense Oligonucleotides. All antisense oligonucleotides were generous gifts from ISIS Pharmaceuticals (Carlsbad, CA) through Dr. C. F. Bennett. The in vivo studies and the rat liver endothelial cell in vitro experiments were carried out with rat anti ICAM-1 antisense sequence, targeting 3′ untranslated region rat ICAM-1 mRNA (ISIS 9125; sequence, 5′-AGGGCCACTGCTCGTCCACA-3′) or its mismatched control (ISIS 13994; sequence, 5′-AGGGCCGCACGTTCTCCACA-3′), both 20-mer phosphorothioate oligodeoxynucleotides. Because the rat targeted sequence ISIS 9125 does not match the murine ICAM-1 mRNA, experiments with J774 cells were performed using phosphorothioate the 20-mer murine anti-ICAM-1 (ISIS 17481–3; sequence, 5′-TCCCACAGCAGCTTGCACGA-3′) and corresponding control (ISIS 20440–2; sequence, 5′-TCCGACAGCACCTTGCACGA-3′) sequences with 2′-*O*-(2-methoxy) ethyl modification at seven nucleotide sugars at the 3′ end. In addition, all the cytosines in ISIS 17481–3 and ISIS 20440–2 were modified to contain a 5-methyl group (5-methyl cytosine).

Animals. Specified pathogen-free male Wag/Rij rats (Harlan, Horst, The Netherlands) were kept under standard animal laboratory conditions and had free access to standard lab chow and water. The studies as presented are in accordance with the Guide for the Care and Use of Laboratory Animals as adopted and promulgated by the U.S. National Institutes of Health and were approved by the local committee for care and use of laboratory animals.

SALP Preparation. Stabilized antisense lipid particles were prepared according to Semple et al. (2001) with slight modifications. POPC, cholesterol, PEG-DSPE, and DOTAP in $CHCl_3$/methanol (9:1) stock solutions were mixed in the molar ratio 3:4:1:2. When used, MPB-PE amounted to 2.5 mol% of the total amount of lipid (TL) at the expense of the amount of POPC. The amount of Mal-PEG-DSPE was 1 mol% of total lipid. When appropriate, 0.25 μCi of [^{3}H]cholesteryl oleyl ether ([^{3}H]COE) per μmol TL was added. The organic solvent was evaporated under nitrogen gas and lipids were redissolved in cyclohexane and freeze-dried overnight. The lipids were dissolved in ethanol 96% shortly before mixing with ODN in buffer containing 10 mM HEPES and 150 mM NaCl (HBS; pH 6.7), resulting in 40% ethanol final concentration. The ODN-to-lipid ratio used was 50 μg of ODN per micromole of total lipid. After vortexing 10 times for 30 s, particles were sized by repeated extrusion (10 times) through polycarbonate membranes with a pore size of 100 nm (Whatman, Maidstone, Kent, UK) before they were extensively dialyzed against HBS, pH 6.7 overnight. Outside-bound ODN was removed by anion exchange chromatography (DEAE).

Coupling of Aco-HSA. *cis*-Aconitylated human serum albumin (Aco-HSA), with an average of 53 of the 60 available ϵ-amino groups derivatized, was prepared as described previously (Kamps et al., 1996). The aconitylated protein was thiolated by means of *N*-succinimidyl-*S*-acetylthioacetate and coupled to either the MPB-PE in the outer surface of the SALPs or to the maleimide group at the distal end of the PEG chain by a sulfhydryl-maleimide coupling technique. Aco-HSA was added to the SALP suspension in a ratio of 0.3 mg/μmol of TL, and the coupling was done within 4 h at room temperature (Derksen and Scherphof, 1985; Kamps et al., 1996). *N*-Ethylmaleimide, 80 mM in buffer, containing 5 mM HEPES, 150 mM NaCl, and 0.1 mM EDTA, pH 7.4, was added to cap unreacted sulfhydryl groups. Protein-coupled SALPs were separated from unconjugated protein by OptiPrep gradient ultracentrifugation. The Aco-HSA coupled SALPs were extensively dialyzed against HBS, pH 7.4. Control SALPs were prepared similarly, except that they were incubated with cysteine, instead of with Aco-HSA, in a molar amount twice that of MPB-PE or PEG-Mal to block reactive maleimide groups. The Aco-HSA SALPs were characterized by determining protein (Peterson, 1977), phospholipid phosphorus and ODN phosphorus content (Böttcher et al., 1961), and ODN content by OliGreen assay. The particle size was determined by dynamic light scattering (Nicomp 380 submicron particle analyzer system; Particle Sizing Systems, Santa Barbara, CA) in the volume-weighing mode. The ζ potential was measured in demineralized water (Nicomp 380). Figure 1 schematically represents the two types of Aco-HSA-coupled SALP preparations: Aco-HSA MPB-PE SALPs and distal end-coupled Aco-HSA Mal-PEG SALPs.

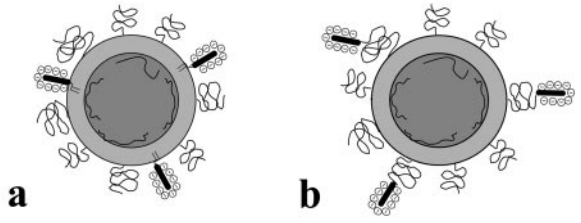

Fig. 1. Schematic representation of proposed models for differently coupled Aco-HSA SALPs. a, Aco-HSA SALPs with Aco-HSA coupled to MPB-PE present at the particle's surface. b, Aco-HSA Mal-PEG SALPs with the homing device coupled to the maleimide group at the distal end of Mal-PEG-DSPE. The diagram is not to scale for all components.

Oligodeoxynucleotide Quantification. ODN entrapped in SALPs was quantified by the OliGreen ssDNA assay (Molecular Probes) according to the manufacturer's protocol and measured in a microtiterplate fluorescence reader (Bio-Tek Instruments, Winooski, VT). To facilitate accessibility of the ODN, SALP samples were diluted into 10 mM Tris-HCl and 1 mM EDTA, pH 7.5, containing 125 μM PS and 165 nM octylglucoside (TE-PS/OG). The ODN calibration standards were diluted in this buffer. Linearity of the standard curve was assured between 0.9 and 18 ng of ODN/ml ($r \geq 0.98$).

Cryotransmission Electron Microscopy. For cryoelectron microscopy studies, high ODN-encapsulating SALPs were separated from SALPs containing little or no ODN, by discontinuous sucrose density gradient centrifugation as described by Zhang et al. (1999). The bands containing SALP were separately isolated by carefully pipetting them off. Fractions were extensively dialyzed against HBS, pH 7.4. The cryotransmission electron micrographs were taken using a Leo 912 Omega electron microscope (Zeiss, Oberkochen, Germany), equipped with a cryotransmission stage. Samples were prepared as described elsewhere (Kaiser et al., 2003).

Animal Studies. For in vivo studies, pentobarbital-anesthetized Wag/Rij rats (200–250 g) were injected with 2 μmol (total lipid) of [^{3}H]COE-labeled SALPs via the penile vein. Blood samples were taken from the inferior vena cava. After 30 min, the liver was perfused and processed for measurement of radioactivity as described previously (Kamps et al., 1996). Total radioactivity in plasma was calculated according to the equation: plasma volume (milliliters) = [0.0219 × body weight (grams)] + 2.66 (Bijsterbosch et al., 1989). When indicated, rats were injected with 5 mg of polyinosinic acid 2 min before injection with SALPs.

Isolation of Liver Cells and Intrahepatic Distribution Studies. Liver endothelial cells (EC) and Kupffer cells were isolated after pronase perfusion and digestion of the hepatocytes, followed by gradient centrifugation and counter flow centrifugal elutriation as described previously (Daemen et al., 1997). Cell numbers in liver suspensions and in the cell fractions were determined microscopically, and radioactivity in each cell fraction was determined as described previously (Kamps and Scherphof, 2003).

Cell Isolation and Culture. For in vitro studies, liver endothelial cells were isolated by collagenase perfusion (0.05%) as described previously (Kamps and Scherphof, 2003). After isolation, liver endothelial cells were cultured in collagen-coated six-well plates in RPMI-1640 medium supplemented with 20% heat-inactivated fetal calf serum, 2 mM L-glutamine, 100 IU/ml penicillin, 100 μg/ml streptomycin, and 10 ng/ml endothelial cell growth factor (Roche Diagnostics) in humidified 5% CO_2/95% air atmosphere. The medium, now containing 10% fetal calf serum, was replaced after 20 h and every 24 h thereafter. Experiments with the cultured cells were performed on the third day after plating, and 24-h incubations with SALPs were started on day 2.

J774 murine macrophage cells were cultured in Dulbecco's modified Eagle's medium containing 10% FCS, 2 mM L-glutamine, 100 IU/ml penicillin, and 100 μg/ml streptomycin in a humidified 5% CO_2/95% air atmosphere. To study the effects of SALPs on ICAM-1 mRNA levels in J774 cells, cells were plated in six-well plates in appropriate cell numbers so that they reached 80% confluence at the day of experiment. After seeding, cells were allowed to settle for 24 h before the SALP incubation period of 24 to 96 h started. Initial dose was 1 μmol of TL (7 μg of ODN) per well and was maintained by adding 0.5 μmol of TL every 24 h. Cells were stimulated by addition of TNF-α, IL-1β, and IFN-γ (20, 10, and 20 ng/ml) 24 h before RNA isolation.

Total RNA Isolation and cDNA Synthesis. Total RNA was extracted from J774 cells and primary liver EC using RNeasy Mini Kit (Qiagen, Hilden, Germany), as recommended by the supplier. Total RNA (1.5 μg) was treated with 2 U of DNase I (Ambion, Austin, Texas) in a volume of 15 μl to remove contaminating DNA (room temperature for 15 min; 65°C for 10 min).

RNA (1 μg) was heated (65°C, 5 min) in the presence of 0.25 μg of random hexamer primers and 2 ng of dNTPs. First-strand cDNA synthesis engaged 200 U of SuperScript III (Invitrogen, Breda, The Netherlands) with 4 μl of 5× first-strand buffer, 1 μl of 0.1 M dithiothreitol, and 40 U of RNaseOUT ribonuclease inhibitor in a total volume of 20 μl.

Real-Time Quantitative Taqman RT-PCR. Quantitative PCR amplifications were performed on an ABI Prism 7900HT Sequence Detection System (Applera Nederland, Nieuwekerk a/d IJssel, The Netherlands). Primers and probe for ICAM-1 (GenBank accession number NM_010493) were developed in house and consisted of unlabeled mRNA-specific primer sets and minor groove binder probes labeled with 6-carboxyfluorescein and a nonfluorescent quencher. Forward primer, ATGGGAATGTCACCACTCTC; reverse primer, GCACCAGAATGATTATAGTCCAGTTATT; minor groove binder probe, CAGTACTGTACCACTCTC; amplicon size, 108 base pairs. Unlabeled primers and probe labeled with the fluorescent reporter dye VIC at the 5′ end and the quencher 6-carboxytetramethylrhodamine at the 3′ end for the housekeeping gene *GAPDH* were obtained from TaqMan Rodent GAPDH Control Reagents (Applied Biosystems).

The PCR step contained 1 μl of the appropriate RT reaction, 10 μl of TaqMan universal PCR master mix (Applied Biosystems), 200 nM primers, and 100 nM TaqMan probe in a final volume of 20 μl. The PCR cycling conditions were 2 min at 50°C, 10 min at 95°C, and 40 two-step cycles of 15 s at 95°C and 60 s at 60°C. All samples were assayed in triplicate.

Relative Quantification of Gene Expression. Relative quantification of the ICAM-1 mRNA levels was done by subtracting the GAPDH C_T (threshold cycle) from the ICAM-1 C_T values ($\Delta C_T = C_{T\ ICAM} - C_{T\ GAPDH}$). After subtracting the $\Delta C_{T\ cont}$ value of the cytokine-stimulated control cells from the samples' $\Delta C_{T\ sample}$ value, the relative ICAM-1 mRNA expression level ratio was expressed by $2^{-(\Delta CT_{sample} - \Delta CT_{cont})}$. Results of different samples of one experiment were normalized with cytokine-stimulated control cells arbitrarily set at 1.

Statistical Analysis. Statistical significance of differences was evaluated by two-tailed unpaired Student's t test. Differences were considered to be significant when $p < 0.05$.

Results

Physicochemical characteristics of SALPs, one with Aco-HSA directly coupled to the liposomal bilayer (Aco-HSA MPB SALPs) and the other with Aco-HSA coupled to the distal end of the PEG chains (Aco-HSA Mal-PEG SALPs) are given in Table 1. The amount of protein coupled to MPB-PE-containing SALPs under standard coupling conditions (room temperature, 4 h) was about 17 μg/μmol of total lipid. Under the same conditions, protein coupling to Mal-PEG SALPs averaged 45 μg/μmol of TL. Lower protein density (18 μg/μmol TL) was achieved by using a lower concentration of Mal-PEG-DSPE (0.5%) and a shorter coupling time (0.5 h). The amounts of encapsulated ODN were similar in both types of SALPs, and other physicochemical properties were comparable.

Further characterization of Aco-HSA MPB SALPs by

TABLE 1
Characterization of Aco-HSA SALPs

	MPB SALPs	Mal-PEG SALPs
Size before coupling (nm ± S.E.M.)	100.5 ± 6.2	89.7 ± 3.6
Size after coupling (nm ± S.E.M.)	150.6 ± 21.0	164.6 ± 45.4
ζ potential before coupling	−7.8 mV	−1.6 mV
ζ potential after coupling	−13.8 mV	−14.0 mV
ODN content (μg/μmol ± S.E.M.)	7.8 ± 3.7	8.1 ± 2.5
Protein (μg/μmol ± S.E.M.)	16.6 ± 0.3	17.9 ± 1.4 (low) 45.1 ± 4.0 (high)

means of cryoelectron microscopy shows size homogeneity of the Aco-HSA SALPs preparation (Fig. 2). SALPs with higher amounts of encapsulated ODN (>50 μg/μmol of TL), as obtained by discontinuous sucrose density gradient centrifugation, have a more electron dense core. Upon prolonged observation in the electron microscope, these dense cores show signs of destruction by the electron beam, consistent with high ODN encapsulation (Frederik et al., 1993).

In Vivo Serum Stability of SALPs. Blood elimination of untargeted stabilized antisense lipid particles containing either Mal-PEG-DSPE or MPB-PE was examined in Wag/Rij rats (Fig. 3). The two types of untargeted SALPs showed comparably slow serum elimination, as measured with [^{3}H]COE (a nondegradable lipid marker) or encapsulated ^{32}P-labeled ODN. After 24 h, 40% of the total injected dose was still present in the blood circulation. Untargeted MPB SALPs were also labeled with ^{32}P-labeled ODN. The identical blood elimination of the lipid label ([^{3}H]COE) and the ODN label (^{32}P) demonstrates that the ODN remained chemically intact and tightly associated with the SALPs during prolonged circulation.

Pharmacokinetics of Aco-HSA SALPs. Aco-HSA SALPs, with the albumin coupled to the bilayer by means of MPB-PE, showed limited blood elimination within 30 min (Fig. 4). Even after 24 h, more than 40% of the total injected dose was still in circulation (data not shown). Aco-HSA SALPs with the albumin coupled to the distal end of the PEG chains were cleared very rapidly, resulting in as little as 5% or less of the injected dose still in circulation after 30 min (Fig. 4), for both the low (15 μg/μmol) and high (45 μg/μmol) protein density preparations. The differences in blood disappearance correlate well with the liver uptake values for the two targeted ODN carrier types (Table 2). After 30 min, the liver took up 80% of the total injected dose of Aco-HSA Mal-PEG SALPs, but for the Aco-HSA MPB SALPs, this was only 10%. No significant differences between high- and low-density-coupled Aco-HSA Mal-PEG SALPs were found in liver uptake and spleen accumulation. The uptake of both Aco-HSA SALP preparations, Mal-PEG and MPB, by hepatic endothelial cells and Kupffer cells was determined after isolation of these cell types (Fig. 5). For Aco-HSA Mal-PEG SALPs, liver endothelial cells accounted for an uptake of as much as 55% of the injected dose, whereas only 7% of the injected dose of MPB-PE coupled Aco-HSA MPB SALPs was taken up by these cells after 30 min. Kupffer cell uptake amounted to 25% of total injected dose with Aco-HSA Mal-PEG SALPs and 2% in the case of Aco-HSA MPB SALPs. Preinjection of polyinosinic acid (5 mg/rat), an established inhibitor of scavenger receptor (ScR)-mediated endocytosis, inhibited liver uptake and liver endothelial cell uptake of both Aco-HSA MPB SALPs and Aco-HAS Mal-PEG SALPs by 70%, confirming the major involvement of the ScR in the uptake process of Aco-HSA-coupled lipid particles (Table 2 and Fig. 5). In this respect, the SALPs behave similarly to what we observed earlier for CCLs (Bartsch et al., 2002).

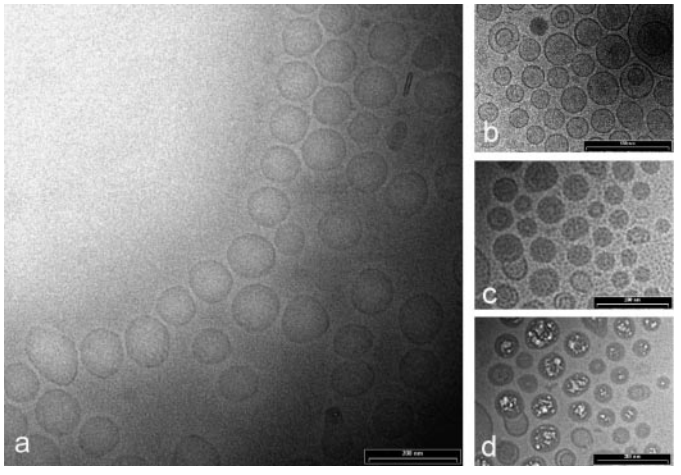

Fig. 2. Cryoelectron micrograph of Aco-HSA MPB SALPs. a, preparation of Aco-HSA MPB SALPs after coupling. b, low ODN encapsulating Aco-HSA MPB SALPs after isolation by sucrose density gradient centrifugation. c, high ODN encapsulating Aco-HSA MPB SALPs after isolation by sucrose density gradient centrifugation showing electron dense core. d, the electron dense cores are vulnerable to electron beam damage during observation, same field as c.

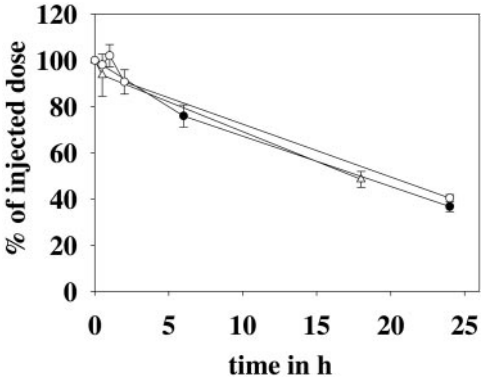

Fig. 3. Serum disappearance of untargeted SALPs. ^{32}P-ODN-labeled MPB SALPs (△, n = 2; error bars indicate range), [^{3}H]COE-labeled MPB SALPs (●, n = 4 ± S.E.M.), and [^{3}H]COE-labeled PEG-Mal SALPs (○, n = 2; error bars indicate range) were injected into anesthetized rats in a dose of 2 μmol TL/rat. Blood samples were taken at indicated time points and radioactivity was determined as described under *Materials and Methods*.

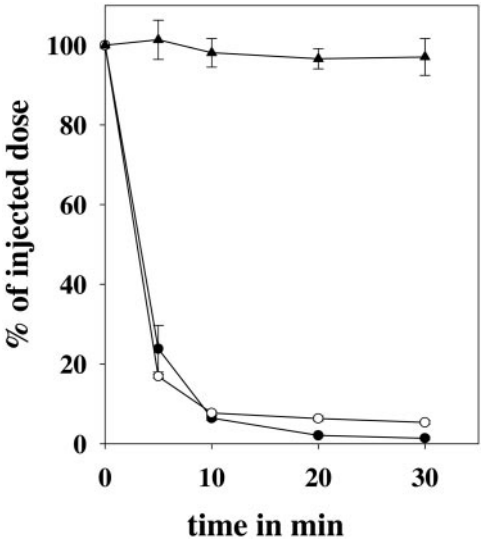

Fig. 4. Serum disappearance of Aco-HSA MPB SALPs and Aco-HSA Mal-PEG SALPs. Aco-HSA MPB SALPs (17 μg/μmol TL, ▲, n = 3 ± S.E.M.), Aco-HSA Mal-PEG SALPs (41 μg/μmol TL, ●, n = 3 ± S.E.M.), or Aco-HSA Mal-PEG SALPs (15 μg/μmol TL, ○, n = 2; error bars indicate range) were injected into anesthetized rats at a dose of 2 μmol of TL/rat. Blood samples were taken at indicated times, and radioactivity was determined as described under *Materials and Methods*.

Interaction of Aco-HSA Coupled SALPs with Anion Exchange Resin. Scavenger receptors require multiple negative charges and sufficient charge density for efficient substrate binding (Jansen et al., 1991; Van Berkel et al., 1991). The multiple negatively charged groups on the derivatized albumin, therefore, probably account for most of the interaction of the Aco-HSA-targeted SALPs with the ScR.

The conspicuous difference in ScR interaction of the bilayer-coupled Aco-HSA and the distal-end coupled Aco-HSA SALP preparations could be mimicked by allowing the two preparations to interact with an anion exchange column. As shown in Fig. 6, a major fraction of the applied amount of Aco-HSA SALPs was eluted without any retention by the anion exchange column in physiological buffer. In contrast, distal end-coupled SALPs were fully retained through interaction with the column. These particles could only be eluted by a high ionic strength buffer (10× concentrated HBS).

In Vitro Uptake Studies. To further substantiate the involvement of ScR in the uptake of targeted SALPs, we determined the effect of polyinosinic acid on in vitro uptake of the particles by isolated liver endothelial cells. Three-day-old cultures of primary liver endothelial cells were incubated for 3 h at a SALP concentration of 80 nmol of TL/ml and 20 μg/ml poly-I, as described under *Materials and Methods*. The uptake of the rapidly cleared PEG distal end-coupled Aco-HSA SALPs was inhibited by 41.6% ± 10.6 S.E.M., but also uptake of the slowly clearing bilayer-coupled particles was strongly inhibited (65% ± 5.81 S.E.M.), indicating that the interaction of these particles is predominantly mediated by the scavenger receptor.

Biological Activity. We determined whether the ODN, taken up by means of ScR-mediated endocytosis, is capable of specifically blocking gene expression. Therefore, cellular ICAM-1 mRNA levels were analyzed by means of quantitative real-time RT-PCR after in vitro incubation with Aco-HSA SALP particles containing an anti-ICAM-1 directed ODN sequence. In in vivo pilot studies, we were able to detect immunohistochemically the up-regulation of ICAM-1 expression in liver endothelial cells upon lipopolysaccharide administration (data not shown). With primary cultured liver endothelial cells, however, up-regulation of ICAM-1 mRNA by a cytokine mixture (rr TNF-α [20 ng/ml], rr IL-1β [10 ng/ml], rr IFN-γ [20 ng/ml]) was not observed. Moreover, we could not observe an effect on the ICAM-1 mRNA levels as a result of incubation with Aco-HSA SALPs with these cells. As an alternative model, we used J774 cells, originally a murine macrophage cell type that expressed both scavenger receptor activity and (cytokine-inducible) ICAM-1 (Keidar et al., 1996; Ruetten et al., 1999). Scavenger receptor-mediated uptake was confirmed by demonstrating that [^{3}H]COE-labeled Aco-HSA liposome uptake could be inhibited in J774 cells by 25 μg/ml polyinosinic acid (data not shown).

The cells were incubated with MPB-PE- or Mal-PEG-DSPE-coupled SALPs for incubation periods varying from 24 to 96 h with a multiple dosing regimen (Fig. 7). Isolated total RNA was analyzed for ICAM-1 gene expression by real-time RT-PCR. No effect on the ICAM-1 mRNA level was observed with unstimulated J774 cells. Addition of the cytokine mixture 24 h before RNA isolation resulted in an 8-fold (± 2.4 S.E.M.) increased ICAM-1 mRNA level compared with untreated cells. Inhibition of cytokine mediated ICAM-1 stimulation was observed in most experiments with the Aco-HSA Mal-PEG SALPs incubations. With 70% reduction of ICAM-1 stimulation, the effect was most profound at 48 h. With bilayer-coupled Aco-HSA SALPs, no consistent effect on ICAM-1 stimulation was observed.

Discussion

When we coupled the negatively charged Aco-HSA directly to the lipid bilayer of MPB-PE containing SALPs by routine procedure, the resulting particles contained 17 μg of protein/μmol of total lipid. These particles were very slowly cleared from circulation, concomitant with negligible uptake by liver endothelial cells. When the polyanionic albumin is coupled in this way, it is probably poorly recognized by the ScR on the endothelial cells, which requires a cluster of negative charges for proper receptor-ligand interaction (Keidar et al., 1996; Ruetten et al., 1999). This interpretation was confirmed by our observation that these particles fail to interact with an anion exchange column. At least two explanations are conceivable for the low ScR interaction of the surface-coupled Aco-HSA SALPs with low (< 20 μg/μmol) protein density: 1) steric shielding of the Aco-HSA groups by the PEG chains, and 2) (partial) neutralization of the negative charge cluster of the Aco-HSA caused by close proximity to the positively charged DOTAP molecules in the particle's bilayer. Earlier (Bartsch et al., 2002), we showed that Aco-HSA-coupled CCLs, which also bear PEG but have a neutral surface, interact readily with the ScR, indicating that the mere presence of the PEG chains is not likely to be a major cause of the lack of interaction of SALPs with ScR. The structure of the CCLs differs from that of SALPs in that the CCLs consist of an inner core containing the cationic lipid DOTAP complexed to ODN, subsequently coated by neutral lipids. This results in a neutral particle surface. In SALPs, on the other hand, the DOTAP is localized, at least in part, in the bilayer encapsulating the ODN and thus confers positive charge to the particle's surface, which may (partly) neutralize the negative charges of the albumin. Hence, we consider the second explanation more likely to cause the strongly reduced interaction between particle and receptor.

To position the Aco-HSA further away from the positively charged surface, the protein was coupled via maleimide

TABLE 2

Biodistribution of Aco-HSA Mal-PEG SALPs and Aco-HSA MPB SALPs with and without preinjection of polyinosinic acid

Serum concentrations and spleen and liver uptake of [^{3}H]COE-labeled Aco-HSA MPB SALPs (17 μg/μmol of TL) and Aco-HSA Mal-PEG SALPs (45 μg/μmol of TL) 30 min after injection into anaesthetized rats in a dose of 2 μmol of TL per rat (n = 3 ± S.E.M.). When indicated, 5 mg of polyinosinic acid (poly I) was injected 2 min before Aco-HSA MPB-PE SALPs and Aco-HSA Mal-PEG SALPs (n = 3 ± S.E.M.). Data are presented as percentage of injected dose.

	Serum	Spleen	Liver
Aco-HSA MPB SALPs	97.1 ± 4.6	2.1 ± 0.9	8.9 ± 3.3
poly I + Aco-HSA MPB SALPs	96.6 ± 9.7	1.4 ± 0.2	2.0 ± 0.6
Aco-HSA Mal-PEG SALPs	1.2 ± 0.3	4.6 ± 0.6	79.3 ± 3.5
poly I + Aco-HSA Mal-PEG SALPs	32.9 ± 18.5	3.7 ± 0.7	26.9 ± 6.8

groups at the distal end of bilayer-anchored PEG-chains. When 0.5 or 1% Mal-PEG-DSPE was added to the lipid mixture, in addition to 10% PEG-DSPE, the average coupling efficiency obtained was 18 μg/μmol (± 1.4 S.E.M.) or 45 μg/μmol TL (± 4.0 S.E.M.), respectively, when our standard coupling conditions were applied. These distal end-coupled Aco-HSA Mal-PEG SALPs interacted avidly with the ScR and anion exchange column and displayed strongly increased targeting potential, irrespective of protein density. Unlike the MPB-coupled Aco-HSA SALPs, Aco-HSA Mal-PEG SALPs showed very rapid serum disappearance: 80% of the injected dose was taken up by the liver within 30 min, and 75% of that was recovered in the endothelial cell fraction. Preinjection of the scavenger receptor inhibitor polyinosinic acid strongly reduced liver uptake, showing that scavenger receptors play a major role in the uptake process. Our attempts to subsequently demonstrate a biological effect of antisense ODN taken up by liver endothelial cells via scavenger receptors were met with limited success. In vitro, ICAM-1 antisense ODN containing Aco-HSA SALPs failed to reduce the ICAM-1 mRNA level in primary liver endothelial cells. Although in preliminary in vivo experiments we had seen that the level of ICAM-1 expression in the liver sinusoid can be up-regulated substantially by lipopolysaccharide, as revealed by immunohistochemistry, liver endothelial cells in primary culture were consistently refractory to up-regulation of ICAM-1 mRNA levels by cytokine treatment. Previous studies have failed to demonstrate marked induction of ICAM-1 in isolated rat hepatocytes as well (F. Bennett and T. Condon, unpublished data). In J774 cells, however, which express both scavenger receptors and ICAM-1, cytokine-mediated ICAM-1 up-regulation was observed. In these cells, we repeatedly achieved reduction of cytokine-stimulated ICAM-1 expression with anti-murine ICAM-1 antisense ODN encapsulated in Aco-HSA Mal-PEG SALPs, although occasionally significant antisense effects was not observed. In contrast, surface-coupled Aco-HSA MPB SALPs, however, consistently showed no effect. Obviously, coupling of the targeting ligand to the distal end of PEG chains on the particles has a beneficial effect on the expression of antisense activity, probably because of enhanced uptake and recognition of the

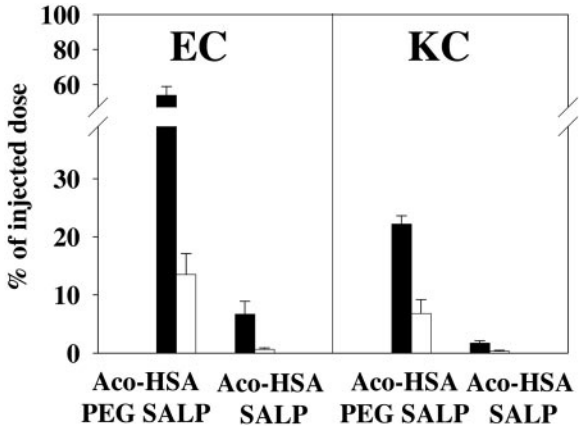

Fig. 5. Intrahepatic distribution of Aco-HSA Mal-PEG SALPs and Aco-HSA MPB SALPs and effect of polyinosinic acid. Uptake by hepatic cell fractions was measured 30 min after injection of Aco-HSA Mal-PEG SALPs and Aco-HSA MPB SALPs into anesthetized rats in a dose of 10 μmol TL/kg bodyweight (■). Uptake by hepatic cell fractions after 30 min, when 5 mg of polyinosinic acid was injected 2 min before Aco-HSA Mal-PEG SALPs and Aco-HSA MPB SALPs (□). Data are calculated as a percentage of total liver uptake, representing means ± S.E.M. of three independent experiments. Hepatic cell isolation and radioactivity determination were performed as described under *Materials and Methods*.

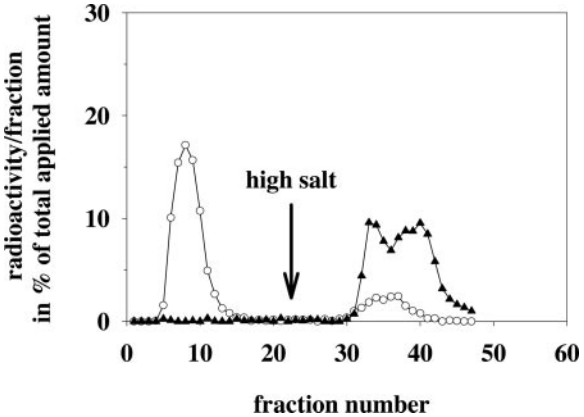

Fig. 6. Interaction of differently targeted SALPs with anion exchange column. [^{3}H]COE-labeled Aco-HSA MPB SALPs (○) or [^{3}H]COE-labeled Aco-HSA Mal-PEG SALPs (▲) were applied to a DEAE column in HBS, pH 7.5, and radioactivity in 1-ml fractions was measured. SALPs were eluted by HBS, pH 7.5 (fraction 1–26) or 10× HBS, pH 7.5 (fraction 27–46).

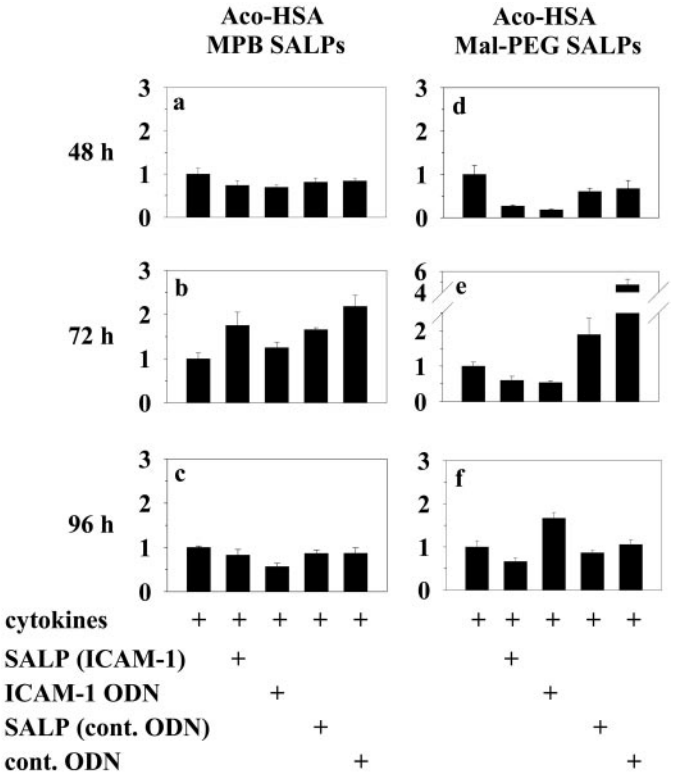

Fig. 7. ICAM-1 mRNA expression in J774 cells after incubation with Aco-HSA MPB SALPs (a–c) or Aco-HSA Mal-PEG SALPs (d–f), determined by real-time RT-PCR analysis. The cells were incubated in six-well plates for 48 h (a and d), 72 h (b and e), or 96 h (c and f) with either targeted SALPs in an initial dose of 1 μmol of TL SALP (= 7 μg ODN) per well and additional 0.5 μmol of TL every 24 h thereafter or with unformulated ODN in an initial dose of 20 μg/well and 10 μg/well every 24 h thereafter. Twenty-four hours before RNA isolation, ICAM-1 expression was stimulated by addition of TNF-α (20 ng/ml), IL-1β (10 ng/ml), and IFN-γ (20 ng/ml). Cells were incubated with ODNs or Aco-HSA SALPs as indicated in the figure. ICAM-1 mRNA levels were quantified as described under *Materials and Methods* and expressed relative to the control cytokine-stimulated cells. Values are means of three analysis ± S.D. (of one experiment).

particles. Unformulated ODN directed against ICAM-1 also exerts antisense activity at early time points. For J774 cells, this has been reported before for other antisense ODNs (Zhu et al., 2002).

The antisense literature is full of conflicting results, partly because of the use of different cell types. However, even within the same cell line, findings can be contradictory. Lucas et al. (2004) observed antisense activity in A549 cells using phosphorothioate ODN and phosphodiester ODN sequences complexed in polyplexes, whereas with the transfection reagent Lipofectin, the same phosphodiester sequence showed no effect but the phosphorothioate sequence did. On the other hand, Leonetti et al. (2001) were able to demonstrate unequivocal antisense activity of SALPs. They showed that untargeted SALPs containing c-myc ODN antisense (INX6295) in vivo substantially down-regulate c-myc in a human melanoma xenograft mouse model, causing reduced tumor growth and an increased survival rate.

Carriers for in vivo application of antisense activity have to display stability to protect their encapsulated nucleic acid from interaction with serum components (Schatzlein, 2001). On the other hand, a prerequisite for efficient transfection activity of nonviral vectors is the ultimate destabilization of the complex and the escape of the ODN from the endocytic compartment into the cytosol after endocytic internalization (Zelphati and Szoka, 1996; Bally et al., 1999; Chirila et al., 2002). The transfection efficacy of antisense particles suitable for in vivo applications is thus a matter of a delicate balance between serum stability and release from the endocytic compartment (Garcia-Chaumont et al., 2000). This will also apply to the intracellular delivery of ODNs by means of the ScR, whose physiological role is to allow efficient uptake and intralysosomal destruction of a variety of substances. Our results show that intracellular delivery of ODN by means of ScR is feasible and under proper conditions may even lead to significant antisense activity.

Unformulated (naked) ODN showed high uptake by liver endothelial cells in vivo by ScR-mediated uptake (Bijsterbosch et al., 1997; Biessen et al., 1998; Graham et al., 2001). In these studies, however, much higher doses were applied than in our study. Nonetheless, these experiments demonstrate that free ODN uptake by EC is substantial, but the specificity is considerably less than that of our targeted SALP. With free ODN, 22% of the injected dose ends up in the EC, whereas with the targeted SALP, 55% of the injected dose ends up in the EC, indicating a 2.5-fold increased targeting efficiency. However, a real antisense activity of unformulated oligonucleotides upon ScR-mediated uptake has not been reported thus far. The advantage of using carrier-mediated delivery, apart from the homing aspect, may be in the mechanism of intracelllular processing of the endocytosed material. Although unformulated ODN is probably very efficiently hydrolyzed in the lysosomal compartment, the presence of certain lipid components in the carrier-ODN complex may facilitate partial release of the ODN from the endosomes into the cytoplasm before complete destruction can take place. The antisense effect displayed by Aco-HSA Mal-PEG SALPs is compatible with that view. As discussed earlier (Bartsch et al., 2002), intervention in the expression of adhesion factors present on liver endothelial cells could be beneficially applied in anti-inflammatory therapies or in the prevention of liver metastases (Scherphof et al., 1997).

In the development of lipid-based ODN carrier for in vivo applications, our present results represent a rare example of the massive targeted delivery of such nonviral vectors to a distinct cell population in the body (Dass, 2002).

Acknowledgments

We gratefully acknowledge the excellent technical assistance of Bert Dontje.

References

Allen TM and Cullis PR (2004) Drug delivery systems: entering the mainstream. *Science (Wash DC)* **303:**1818–1822.
Bally MB, Harvie P, Wong FM, Kong S, Wasan EK, and Reimer DL (1999) Biological barriers to cellular delivery of lipid-based DNA carriers. *Adv Drug Deliv Rev* **38:**291–315.
Bartsch M, Weeke-Klimp AH, Meijer DKF, Scherphof GL, and Kamps JAAM (2002) Massive and selective delivery of lipid-coated cationic lipoplexes of oligonucleotides targeted in vivo to hepatic endothelial cells. *Pharm Res (NY)* **19:**676–680.
Biessen EA, Vietsch H, Kuiper J, Bijsterbosch MK, and Berkel TJ (1998) Liver uptake of phosphodiester oligodeoxynucleotides is mediated by scavenger receptors. *Mol Pharmacol* **53:**262–269.
Bijsterbosch MK, Manoharan M, Rump ET, de Vrueh RL, Van Veghel R, Tivel KL, Biessen EA, Bennett CF, Cook PD, and Van Berkel TJ (1997) In vivo fate of phosphorothioate antisense oligodeoxynucleotides: predominant uptake by scavenger receptors on endothelial liver cells. *Nucleic Acids Res* **25:**3290–3296.
Bijsterbosch MK, Ziere GJ, and Van Berkel TJ (1989) Lactosylated low density lipoprotein: a potential carrier for the site-specific delivery of drugs to Kupffer cells. *Mol Pharmacol* **36:**484–489.
Böttcher CJF, Van Gent CM, and Pries C (1961) A rapid and sensitive sub-micro phosphorus determination. *Analytica Chimica Acta* **24:**204–205.
Chirila TV, Rakoczy PE, Garrett KL, Lou X, and Constable IJ (2002) The use of synthetic polymers for delivery of therapeutic antisense oligodeoxynucleotides. *Biomaterials* **23:**321–342.
Daemen T, Velinova M, Regts J, de Jager M, Kalicharan R, Donga J, van der Want JJ, and Scherphof GL (1997) Different intrahepatic distribution of phosphatidylglycerol and phosphatidylserine liposomes in the rat. *Hepatology* **26:**416–423.
Dass CR (2002) Liposome-mediated delivery of oligodeoxynucleotides in vivo. *Drug Deliv* **9:**169–180.
Derksen JTP and Scherphof GL (1985) An improved method for the covalent coupling of proteins to liposomes. *Biochim Biophys Acta* **814:**151.
Frederik PM, Bomans PHH, and Stuart MCA (1993) Matrix effects and the induction of mass loss or bubbling by the electron beam in vitrified hydrated specimens. *Ultramicroscopy* **48:**107–119.
Garcia-Chaumont C, Seksek O, Grzybowska J, Borowski E, and Bolard J (2000) Delivery systems for antisense oligonucleotides. *Pharmacol Ther* **87:**255–277.
Graham MJ, Crooke ST, Lemonidis KM, Gaus HJ, Templin MV, and Crooke RM (2001) Hepatic distribution of a phosphorothioate oligodeoxynucleotide within rodents following intravenous administration. *Biochem Pharmacol* **62:**297–306.
Jansen RW, Molema G, Harms G, Kruijt JK, Van Berkel TJ, Hardonk MJ, and Meijer DK (1991) Formaldehyde treated albumin contains monomeric and polymeric forms that are differently cleared by endothelial and kupffer cells of the liver: evidence for scavenger receptor heterogeneity. *Biochem Biophys Res Commun* **180:**23–32.
Kaiser N, Kimpfler A, Massing U, Burger AM, Fiebig HH, Brandl M, and Schubert R (2003) 5-Fluorouracil in vesicular phospholipid gels for anticancer treatment: entrapment and release properties. *Int J Pharm* **256:**123–131.
Kamps JAAM, Morselt HW, Swart PJ, Meijer DKF, and Scherphof GL (1997) Massive targeting of liposomes, surface-modified with anionized albumins, to hepatic endothelial cells. *Proc Natl Acad Sci USA* **94:**11681–11685.
Kamps JAAM and Scherphof GL (2003) Liposomes in biological systems, in *Liposomes, a Practical Approach* (Torchilin VP and Weissig V eds) pp 267–288, Oxford University Press, Oxford.
Kamps JAAM, Swart PJ, Morselt HW, Pauwels R, De Bethune MP, De Clercq E, Meijer DKF, and Scherphof GL (1996) Preparation and characterization of conjugates of (modified) human serum albumin and liposomes: drug carriers with an intrinsic anti-HIV activity. *Biochim Biophys Acta* **1278:**183–190.
Keidar S, Kaplan M, and Aviram M (1996) Angiotensin II-modified LDL is taken up by macrophages via the scavenger receptor, leading to cellular cholesterol accumulation. *Arterioscler Thromb Vasc Biol* **16:**97–105.
Kurreck J (2003) Antisense technologies. Improvement through novel chemical modifications. *Eur J Biochem* **270:**1628–1644.
Leonetti C, Biroccio A, Benassi B, Stringaro A, Stoppacciaro A, Semple SC, and Zupi G (2001) Encapsulation of C-myc antisense oligodeoxynucleotides in lipid particles improves antitumoral efficacy in vivo in a human melanoma line. *Cancer Gene Ther* **8:**459–468.
Lucas B, Van Rompaey E, Remaut K, Sanders N, De Smedt SC, and Demeester J (2004) On the biological activity of anti-ICAM-1 oligonucleotides complexed to non-viral carriers. *J Control Release* **96:**207–219.
Matteucci MD and Wagner RW (1996) In pursuit of antisense. *Nature (Lond)* **384:**20–22.
Opalinska JB and Gewirtz AM (2002) Nucleic-acid therapeutics: basic principles and recent applications. *Nat Rev Drug Discov* **1:**503–514.
Peterson GL (1977) A simplification of the protein assay method of Lowry et al. which is more generally applicable. *Anal Biochem* **83:**346–356.
Pirollo KF, Rait A, Sleer LS, and Chang EH (2003) Antisense therapeutics: from theory to clinical practice. *Pharmacol Ther* **99:**55–77.

Ruetten H, Thiemermann C, and Perretti M (1999) Upregulation of ICAM-1 Expression on J774.2 macrophages by endotoxin involves activation of NF-KappaB but not protein tyrosine kinase: comparison to induction of INOS. *Mediators Inflamm* **8:**77–84.
Schatzlein AG (2001) Non-viral vectors in cancer gene therapy: principles and progress. *Anticancer Drugs* **12:**275–304.
Scherer LJ and Rossi JJ (2003) Approaches for the sequence-specific knockdown of MRNA. *Nat Biotechnol* **21:**1457–1465.
Scherphof GL, Kamps JAAM, and Koning GA (1997) In vivo targeting of surface-modified liposomes to metastatically growing colon carcinoma cells and sinusoidal endothelial cells in rat liver. *J Liposome Res* **7:**419–432.
Semple SC, Klimuk SK, Harasym TO, Dos SN, Ansell SM, Wong KF, Maurer N, Stark H, Cullis PR, Hope MJ, et al. (2001) Efficient encapsulation of antisense oligonucleotides in lipid vesicles using ionizable aminolipids: formation of novel small multilamellar vesicle structures. *Biochim Biophys Acta* **1510:**152–166.
Stuart DD, Semple SC, and Allen TM (2004) High efficiency entrapment of antisense oligonucleotides in liposomes. *Methods Enzymol* **387:**171–188.
Van Berkel TJ, De Rijke YB, and Kruijt JK (1991) Different fate in vivo of oxidatively modified low density lipoprotein and acetylated low density lipoprotein in rats. Recognition by various scavenger receptors on Kupffer and endothelial liver cells. *J Biol Chem* **266:**2282–2289.
Zelphati O and Szoka FC Jr (1996) Mechanism of oligonucleotide release from cationic liposomes. *Proc Natl Acad Sci USA* **93:**11493–11498.
Zhang YP, Sekirov L, Saravolac EG, Wheeler JJ, Tardi P, Clow K, Leng E, Sun R, Cullis PR, and Scherrer P (1999) Stabilized plasmid-lipid particles for regional gene therapy: formulation and transfection properties. *Gene Ther* **6:**1438–1447.
Zhou W, Yuan X, Wilson A, Yang L, Mokotoff M, Pitt B, and Li S (2002) Efficient intracellular delivery of oligonucleotides formulated in folate receptor-targeted lipid vesicles. *Bioconjug Chem* **13:**1220–1225.
Zhu FG, Reich CF, and Pisetsky DS (2002) Inhibition of murine macrophage nitric oxide production by synthetic oligonucleotides. *J Leukoc Biol* **71:**686–694.

Address correspondence to: Jan A. A. M. Kamps, University of Groningen, Department Pathology and Laboratory Medicine/Medical Biology Section - Endothelial Cell Research and Vascular Drug Targeting, Hanzeplein 1, 9713 GZ Groningen, The Netherlands. E-mail: j.a.a.m.kamps@med.rug.nl